Motion and metacontrast with simultaneous onset of stimuli

Walter F. Bischof and Vincent Di Lollo

Department of Psychology, University of Alberta, Edmonton, Alberta T6G 2E9, Canada

Received September 2, 1994; revised manuscript received March 14, 1995; accepted March 14, 1995

Coherent directional motion can be seen if an image is displayed in two sequential frames (F1 and F2), where F2 is a translated version of F1. A similar two-frame sequence can produce metacontrast masking: the visibility of a leading target (F1) is reduced by a trailing, spatially nonoverlapping mask (F2). Strict temporal succession of the stimuli has been considered essential for both motion and masking. This requirement for a minimum stimulus-onset asynchrony (SOA) is known as the SOA law. Contrary to the SOA law, we found that motion and masking can be obtained with simultaneous onsets of the stimuli, provided that F2 outlasts F1. We compared motion and metacontrast with simultaneous onsets of the stimuli (SIM paradigm) with the traditional paradigm in which an interstimulus interval (ISI) is inserted between the leading and the trailing stimuli (ISI paradigm). We studied the effects in light-adapted and in dark-adapted viewing, each over a wide range of stimulus intensities. Homologous results were obtained with the two paradigms, thus disconfirming the SOA law. Models of motion sensors, such as that proposed by Reichardt [in *Sensory Communication,* W. A. Rosenblith, ed. (MIT Press, Cambridge, Mass., 1961), p. 303], are inherently capable of explaining the motion results obtained with both paradigms. The masking results with the SIM paradigm disconfirm theories based on onset-locked slow excitatory and fast inhibitory responses but can be explained in terms of Bridgeman's network model [Bull. Math. Biol. **40,** 605 (1978)]. In light of the results obtained with the two paradigms, we discuss, and tentatively support, the suggestion that motion and metacontrast may be complementary parts of a unitary perceptual system.

Brief visual stimuli displayed sequentially in adjoining spatial locations can give rise to at least two well-known perceptual phenomena: apparent motion and metacontrast masking. In apparent motion the stimuli are displayed in two sequential frames separated by a temporal gap [interstimulus interval (ISI)] during which the screen remains blank. The leading frame (F1) may consist of a set of dots distributed randomly on the display surface; the trailing frame (F2) is the same as F1 except that each dot has been displaced by a fixed extent in a uniform direction. Under appropriate spatiotemporal conditions the dots are seen as moving in the direction of the spatial displacement. A similar temporal sequence is used in metacontrast masking: in this case, F1 is a target (e.g., a disk) to be identified or rated by the observer and F2 is a mask (e.g., an annulus) with contours close to the target. Under appropriate spatiotemporal conditions the visibility of the target is reduced by the trailing mask.

There has been general agreement that strict temporal succession is essential in both paradigms. That is, for motion or metacontrast to be perceived, F1 must precede F2 by some temporal interval. The required temporal separation can be achieved by insertion of an ISI between F1 and F2 or, with ISI equal to zero, by display of F1 continuously until the onset of F2. In either case the crucial variable is held to be not the ISI but stimulus-onset asynchrony (SOA), the interval between the two onsets.[1] Because of its stability, this temporal relationship has come to be known as the onset–onset law[2] or the SOA law.[3]

We have found that, contrary to the SOA law, strict temporal succession is not a necessary condition for motion or metacontrast.[4] That is, motion and metacontrast can be obtained with simultaneous onsets of F1 and F2 (i.e., with SOA equal to zero), provided that F2 outlasts F1 by a suitable margin. This finding is of considerable practical and theoretical interest, especially for inhibitory theories of metacontrast masking. In an earlier paper[4] we showed that computational models of motion sensors are inherently capable of encompassing this result because the generation of a motion signal is predicated on a transient energy imbalance that is not necessarily time locked to stimulus onset. By contrast, this result cannot be handled by inhibitory theories of metacontrast predicated on slow excitatory and fast inhibitory processes that are time locked to stimulus onset.

The present study was designed to explore some of the limiting conditions of motion and metacontrast with simultaneous onset (SIM) of the stimuli. The work had two major objectives: first, to compare directly the effects obtained by use of the new SIM paradigm with the corresponding effects obtained by use of the traditional paradigms in which the stimuli are presented in strict temporal succession and, second, to examine the two phenomena over a range of stimulus intensities in light-adapted and dark-adapted viewing.

1. MOTION

Directional motion perception was studied with two distinct paradigms. For convenience we denote the two paradigms with reference to the temporal relationship between the onsets of the stimuli. In the ISI paradigm a variable ISI elapsed between F1 and F2 during which the screen remained blank; the exposure duration of F1 was

0740-3232/95/081623-14$06.00

1 ms, as was that of F2. In the SIM paradigm, F1 and F2 were displayed simultaneously for 1 ms; then F1 was turned off and F2 remained on view for a period that matched the duration of the ISI in the corresponding condition in the other paradigm. In both paradigms the intensity of the stimuli was varied over a wide range in both dark-adapted and light-adapted viewing.

A. Methods

1. Observers and Apparatus

Two male students served as observers. Both had normal uncorrected vision. Stimuli were groups of dots (described further below) displayed on a Tektronix 608 oscilloscope equipped with a P15 phosphor. The *X*, *Y*, and *Z* (intensity) coordinates of each dot were stored in a fast plotting buffer that transferred them to the screen at the rate of 1 dot/μs.[5] The intensity of the dots was measured with a Minolta LS-110 luminance meter following the method described by Sperling.[6] Values of luminous directional energy (LDE) were expressed in millicandela microseconds (mcd μs) rather than in candela microseconds, as commonly used, to avoid very small numbers.

Images were displayed within a square area in the center of the screen. At a viewing distance of 57 cm, set by a headrest, the square area subtended an angle of 2°. When required, the screen was front illuminated with a Kodak Carousel projector equipped with a 500-W GE Quartzline projection lamp, attenuated to the required luminance by neutral-density filters. Observers sat in a lightproof observation room and viewed the display with natural pupils.

2. Viewing Conditions

Four basic viewing conditions were defined in terms of the factorial combination of two paradigms (ISI and SIM) and two levels of luminance (dark adapted and light adapted). Within each viewing condition, duration of ISI and the intensity of dots were varied as described below.

ISI Dark-Adapted Condition. The observer was dark adapted for a minimum of 30 min before the beginning of each experimental session. All stimuli were displayed on a dark screen. On every trial the following apparent-motion sequence was displayed: first, a set of 40 dots (F1), distributed randomly over the 2 × 2° viewing area, was displayed for 1 ms. The size of each dot was approximately 0.25 arcmin. Next there was an ISI of 0, 9, 19, 39, 79, or 159 ms during which the screen remained blank. Given that the duration of F1 was 1 ms, these ISI's corresponded to SOA's of 1, 10, 20, 40, 80, and 160 ms. Finally, a second set of dots (F2) was displayed for 1 ms. F2 was identical to F1 except for a uniform horizontal displacement of 10 arcmin of all the dots. The direction of displacement (left or right) was chosen randomly on each trial. The displacement occurred entirely within the spatial confines of the 2° × 2° viewing area with conventional wraparound for dots displaced outside the viewing area. Luminance of the dots was set separately for each observer so as to cover a range that yielded accuracy of performance from just above chance level to asymptotic level. At the lowest intensity the dots were above absolute threshold but barely visible. Thus dots with an LDE of ~50 mcd μs were just above detection threshold (see, e.g., Fig. 1 below).

On each trial the sequence of events was as follows: a dim fixation cross (0.5° × 0.5°) was displayed in the center of the screen. When ready, the observer pressed a push button on a hand-held box to initiate a trial. When the button was pressed, the fixation cross disappeared, and after a 200-ms delay the appropriate sequence of stimuli was displayed. Next, the observer reported (or guessed) the direction of motion (left or right) by pressing the appropriate button on the box. Finally, the fixation cross reappeared to indicate readiness for the next trial. An experimental session lasted ~2 h, the first 30 min of which were spent waiting for dark adaptation. Each observer contributed 100 observations for each luminance/ISI combination.

ISI Light-Adapted Condition. Procedures in the ISI light-adapted condition were the same as in the dark-adapted condition, with the following exceptions. Screen illumination was 50 cd/m^2. The preliminary procedures for establishing the range of stimulus intensities were the same as in the dark-adapted condition except that they were carried out with a screen illumination of 50 cd/m^2; therefore the absolute luminance values were higher, as indicated in the legends of the relevant figures.

SIM Dark-Adapted Condition. The SIM dark-adapted condition was the same as the ISI dark-adapted condition, with the following exceptions. All trials began with a simultaneous display of F1 and F2. After 1 ms, F1 was turned off and F2 remained on view for 0, 10, 20, 40, 80, or 160 ms. In the condition in which the additional duration of F2 was 0 ms (i.e., when F1 and F2 started and ended together) the display consisted of, and was seen as, 40 pairs of stationary dots. The preliminary procedures for establishing the range of stimulus intensities were essentially the same as in the ISI conditions except for one additional consideration. Stimuli of different durations were equalized for brightness with a procedure similar to that described by Servière *et al.*[7] and by Di Lollo and Finley.[8] Brightness equalization was introduced for two reasons: first, it eliminates possible confounds that are due to stimulus visibility[9] or to brightness mismatch.[10] Second, it ensures that both the magnitude[11] and the latency[7,9] of the visual response remain constant for stimuli of different durations.

SIM Light-Adapted Condition. The SIM light-adapted condition was the same as the SIM dark-adapted condition except that screen illumination was 50 cd/m^2. Preliminary procedures for establishing the range of stimulus intensities and brightness equalization were the same as for the SIM dark-adapted condition except that they were carried out with a screen illumination of 50 cd/m^2.

A caveat is in order regarding the term dark-adapted. The stimuli were foveal, thus stimulating a virtually rod-free area. The term dark-adapted is meant to describe the adaptation state of the observers and does not imply that perception was mediated exclusively by rods. Mediation by cones may have been possible through rapid light adaptation, especially following the more intense stimuli.[12–14] This, however, does not imply a retinal locus for the results; indeed, we believe that locus to be cortical.

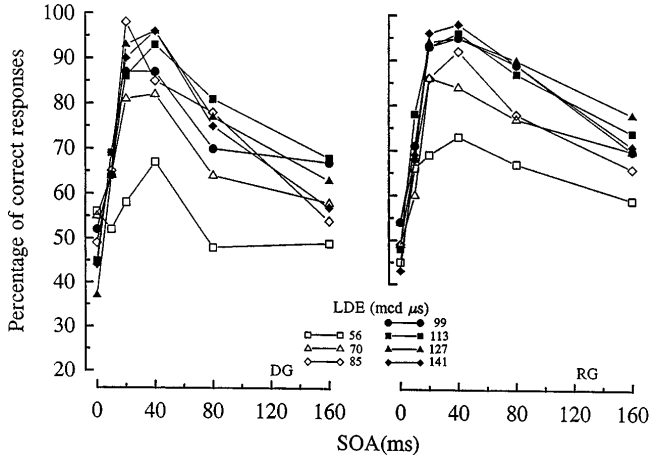

Fig. 1. Motion task, ISI paradigm. Accuracy of detecting directional motion in light-adapted viewing for observers DG and RG. The duration of leading and trailing stimuli was 1 ms. Levels of stimulus intensity are shown in the legend. Chance level was 50%.

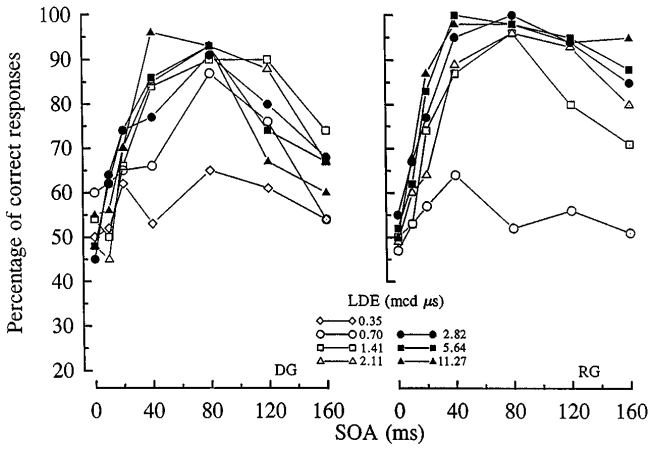

Fig. 2. Motion task, ISI paradigm. Accuracy of detecting directional motion in dark-adapted viewing for observers DG and RG. The duration of leading and trailing stimuli was 1 ms. Levels of stimulus intensity are shown in the legend. Change level was 50%.

B. Results

1. ISI Conditions

Results for the ISI light-adapted condition are shown in Fig. 1, separately for the two observers DG and RG. The corresponding results for the ISI dark-adapted condition are shown in Fig. 2. The effect of the ISI (or, equivalently, of the SOA) was distinctly nonmonotonic in both light-adapted and dark-adapted viewing. That is, detection of coherent directional motion was best at intermediate ISI's and poorer at shorter or longer ISI's. The phenomenological appearance of the displays suggests that the impairment at short and long ISI's was probably mediated by different mechanisms. When the ISI was too long, F1 and F2 tended to be seen as independent, temporally disjoint stimuli that produced no impression of motion. By contrast, when the ISI was too short, F1 and F2 were seen as temporally integrated into a unitary pattern consisting of stationary pairs of dots. It must be stressed that such temporal integration occurred within the visual system, not on the oscilloscope's surface: the use of P15 rules out phosphor persistence as a basis for temporal integration, even over ISI's as brief as 1 ms.[15]

Perception of motion as a function of ISI followed different temporal courses in light-adapted and dark-adapted viewing, as illustrated in Fig. 3. In essence, the curves in Fig. 3 illustrate asymptotic performance with respect to stimulus luminance in light-adapted and dark-adapted viewing. The light-adapted curves in Fig. 3 were obtained by averaging the curves for the two highest luminance conditions in Fig. 1 (127 and 141 mcd μs) separately for each observer. Similarly, the dark-adapted curve for observer RG is the average of the curves for 5.64 and 11.27 mcd μs in Fig. 2. For observer DG, however, the dark-adapted curve is the average of the curves for 1.41 and 2.11 mcd μs in Fig. 2. This was done because, at the longer ISI's, RG's performance was actually lower with more intense stimuli (Fig. 2, left-hand panel). We ascribe this decline to rapid light adaptation,[13] which is known to take place at approximately these ISI's and to be characterized by large individual differences.[16] We deem DG's curves for 1.41 and 2.11 mcd μs to be more representative of his asymptotic performance in dark-adapted viewing.

It is readily apparent from Fig. 3 that ISI interacts with adapting luminance in determining the perceptibility of motion: at short ISI's, the probability of seeing motion is higher in the light than in the dark, but the reverse is true at long ISI's. The former effect corresponds to the observation that F1 and F2 are seen as a single stationary display over longer SOA's in dark-adapted than in light-adapted viewing. The latter effect had been reported in earlier investigations.[17,18] Both effects can be explained in terms of a shift in sensitivity toward the lower temporal frequencies as the state of the visual system changes from light adapted to dark adapted; it is known that the peak of the temporal modulation transfer function shifts toward the lower frequencies as retinal illuminance is decreased.[19,20] Dawson and Di Lollo[17]

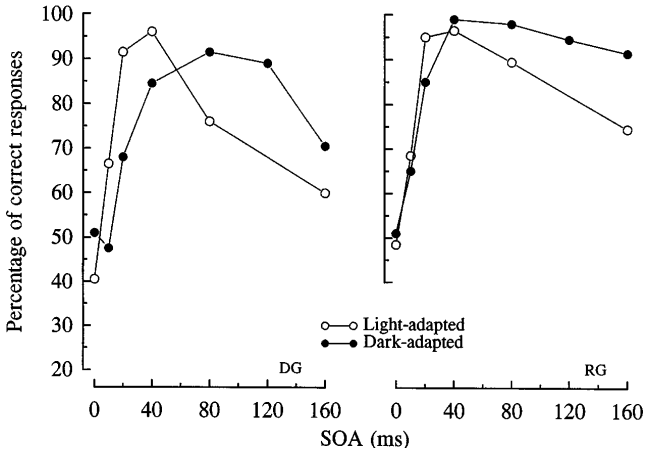

Fig. 3. Motion task, ISI paradigm. Accuracy of detecting directional motion in light-adapted and dark-adapted viewing. Chance level was 50%. The light-adapted curves were obtained by averaging the curves for the two highest stimulus intensities (127 and 141 mcd μs) in Fig. 1, for observers DG and RG. Each dark-adapted curve was obtained by averaging two curves in Fig. 2 as follows: observer DG (1.41 and 2.11 mcd μs); observer RG (5.64 and 11.27 mcd μs).

have shown this pattern of results to be easily explained on the basis of motion sensors of the Reichardt type, described below.

Stimulus luminance acted as a limiting factor on the perceptibility of motion: as is evident from Figs. 1 and 2, the probability of seeing motion increased with stimulus luminance. Improvements in performance with increasing stimulus luminance were due, in all likelihood, to corresponding increments in contrast. The rapid saturation of the effect, especially notable in dark-adapted viewing, is consistent with the rapid saturation known to occur in the motion system with respect to contrast.[21,22] It is important to note that the visibility of the stimuli was never in question in any of the experimental conditions. Indeed, the stimuli were still visible when displayed at luminances below the lowest employed in the present studies. When that was done, however, no motion was seen, regardless of the ISI.

2. SIM Conditions

Results for the SIM light-adapted and the SIM dark-adapted conditions are shown in Figs. 4 and 5, respectively, separately for the two observers. On trials in which F1 and F2 started and ended together, the display consisted of 40 pairs of stationary dots that seemed to remain on view for much longer than 1 ms. Motion was seen with increasing probability as the duration of F2 was increased. The direction of motion was always from F1 to F2; motion was smooth, of excellent quality, and indistinguishable from that seen with the ISI paradigm. At durations of F2 below ~40 ms (80 ms in the dark) the F1 dots were still visible even when motion was seen. At longer durations of F2, the F1 dots were never perceived: only F2 dots were seen, in smooth coherent motion.

To facilitate comparison between the two paradigms, we constructed Fig. 6 to parallel Fig. 3. In Fig. 6 the light-adapted curves are averages of the two highest-luminance conditions in Fig. 4; the dark-adapted curves were obtained in a similar manner from Fig. 5.

Two differences are readily noticed between the results obtained with the ISI and the SIM paradigms. First, the probability of seeing motion declined at the longer ISI's (Figs. 1 and 2) but not at the longer durations of F2 (Figs. 4 and 5). Second, perception of motion followed different time courses in light-adapted and in dark-adapted viewing as a function of ISI (Fig. 3) but not as a function of F2 duration (Fig. 6). These differences are explained below.

C. Discussion

Motion perception with simultaneous onsets of the stimuli contradicts the SOA law: strict temporal succession is not required for perception of motion. Instead, we suggest that motion is seen whenever an energy imbalance occurs in the spatiotemporal spectrum. Just such an imbalance is inherent in the functioning of extant models of peripheral motion-sensing mechanisms such as the sensor first proposed by Reichardt.[23] Below we show how motion sensors of the Reichardt type, activated by an imbalance in the spatiotemporal spectrum, are capable of accounting for the outcomes obtained with both the ISI and the SIM paradigms.

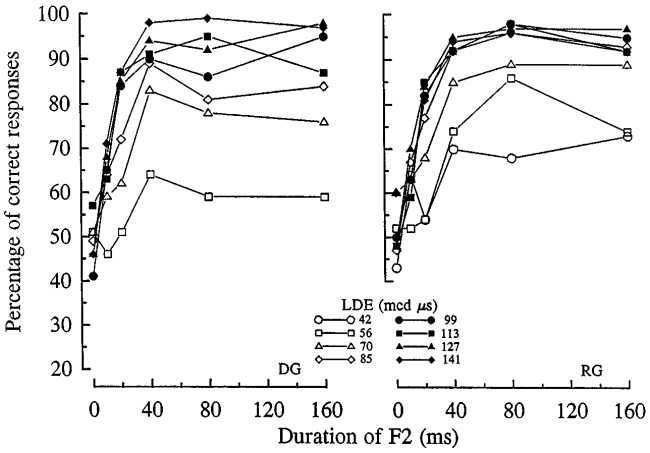

Fig. 4. Motion task, SIM paradigm. Accuracy of detecting directional motion in light-adapted viewing for observers DG and RG. The duration of the initial combined display of F1 and F2 was 1 ms. The duration of the trailing display, F2, indicated on the abscissas does not include the initial 1-ms period. Chance level was 50%.

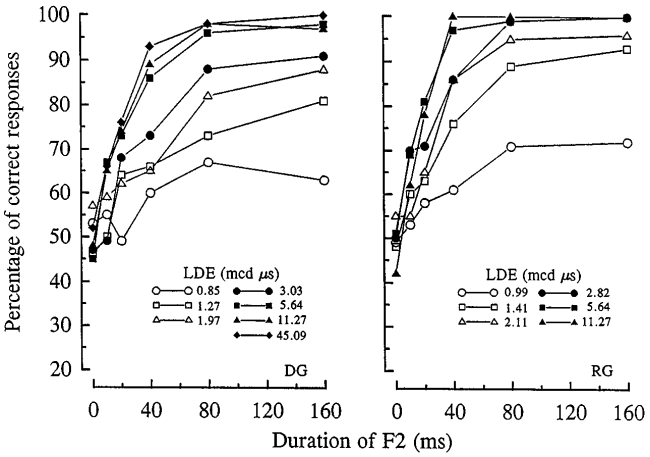

Fig. 5. Motion task, SIM paradigm. Accuracy of detecting directional motion in dark-adapted viewing for observers DG and RG. The duration of the initial combined display of F1 and F2 was 1 ms. The duration of the trailing display, F2, indicated on the abscissas does not include the initial 1-ms period. Chance level was 50%.

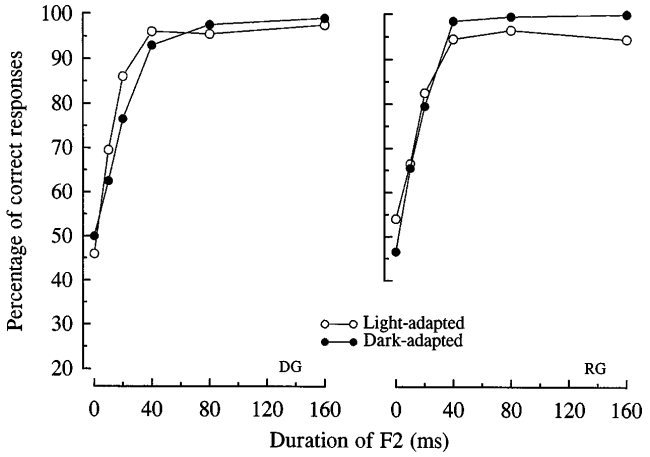

Fig. 6. Motion task, SIM paradigm. Accuracy of detecting directional motion in light-adapted and dark-adapted viewing for observers DG and RG. The light-adapted curves are averages of the two highest luminance conditions in Fig. 4; the dark-adapted curves are similar averages from Fig. 5. Chance level was 50%.

1. Reichardt-Type Motion Sensor

Illustrated in the lower row of Fig. 7 is a Reichardt motion sensor.[23] Signals from two spatially separate inputs travel along two pathways: one is a direct link to an ipsilateral correlator (left, L, or right, R); the other is an indirect link to a contralateral correlator through a delay unit that retards the signal by Δ ms. Each correlator combines the direct and the delayed signals by multiplying them together. From the correlators, the signals converge to the final stage Σ, where they are subtracted one from the other (R minus L) to produce a motion signal. If the sum is positive, rightward motion is signaled; if it is negative, motion is to the left; if it is zero, no motion is detected.

In the elaborated version,[24,25] inputs to the motion sensor are passed through spatial and temporal filters. Especially relevant to the present scheme are the temporal filters. They act to represent the sluggishness of the visual system's response to brief stimuli. That sluggishness is particularly notable with respect to stimulus termination: given a brief display (e.g., 10 ms), the contents of the display remain visible for some time (e.g., 100 ms) after the physical stimulus has terminated. The additional period of visibility, known as visible persistence, has been investigated intensively in recent years.[26–28]

In the present paper we have used Sperling and Sondhi's model[29] to characterize the temporal filter. According to this model, the temporal response changes in two important ways as the state of the visual system changes from light adapted to dark adapted. The shape changes from biphasic to monophasic, and the temporal extent of the positive phase increases apace. The negative phase of the response function has been held to represent inhibitory processes that are weak or absent in dark-adapted vision.[30–33] The positive phase has been held to represent the burst of excitatory activity triggered by the stimulus and has been treated as an index of visible persistence.[29–34]

2. Motion with the ISI Paradigm

Figure 7 shows how a motion sensor of the Reichardt type can account for rightward motion in the ISI paradigm. The SOA between F1 and F2 is assumed to be Δ ms, corresponding to the optimal delay for the sensor. Figure 7(a) shows the status of the motion sensor at time t, namely, the time when an F1 dot is presented to the input unit on the left, resulting in activation of the pathways indicated by filled arrows. At this time, neither correlator is active, the inputs to the final stage are balanced, and no motion signal is produced. Figure 7(b) shows the status of the sensor during the ISI: the delay unit on the left is active but has yet to produce an output. Figure 7(c) shows the status of the sensor at time $t + \Delta$, the time when an F2 dot is presented to the input unit on the right. At this time, the product of the inputs to correlator R is nonzero, so the correlator produces an output. The inputs to the final stage are thus unbalanced, and a rightward-motion signal is issued.

We simulated this sequence of events at five levels of retinal illuminance (from 0.1 to 1000 Td, in steps of 1 log unit). The value of the sensor's delay, Δ, was set at 20 ms. In the simulation our intent was not to provide a quantitative fit to the empirical data but to present a qualitative illustration of the performance curves that might be obtained in light-adapted and dark-adapted viewing from the stimulus sequence shown in Fig. 7. The simulated curves, shown in Fig. 8, are in good qualitative agreement with the empirical curves in Fig. 3. Both the simulated and the empirical curves for light-adapted viewing rise and decline faster than the corresponding curves for dark-adapted viewing.

The theoretical curves in Fig. 8 illustrate changes in the strength of the motion signal as a function of background luminance. In principle, the same can be done

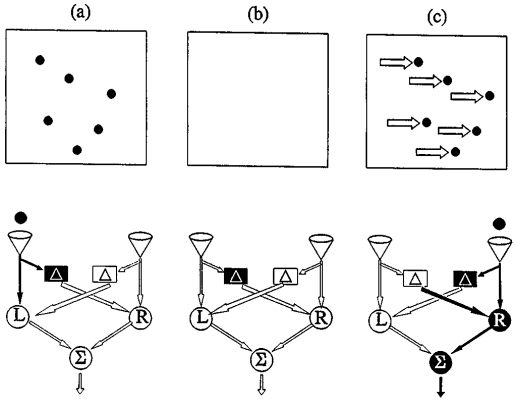

Fig. 7. Schematic representation of a rightward-motion sequence in the ISI paradigm. Filled sections indicate active elements of the motion sensor. (a) Status of the motion sensor on presentation of the leading frame, F1, showing balanced (zero) input to the final stage Σ and no motion signal. (b) Status of the sensor during the ISI; the delay unit on the left is active but is yet to produce an output. (c) Status of the sensor on presentation of the trailing frame, F2, assuming that the duration of the ISI is approximately equal to the period of the sensor's delay Δ; the inputs to the final stage Σ are unbalanced, and a rightward-motion signal is generated.

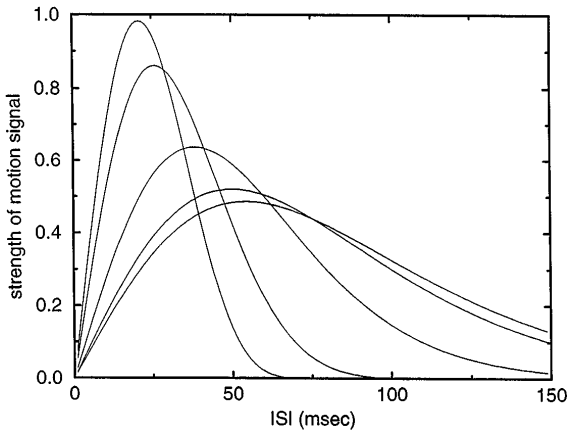

Fig. 8. Peak response of a Reichardt-type motion sensor to the motion stimuli used in the ISI paradigm for a range of ISI's and five levels of retinal illuminance (from 0.1 to 1000 Td, in steps of 1 log unit). At high retinal illuminance a strong motion signal is generated at short ISI's (of the order of 25 ms), but no motion signal is generated at ISI's exceeding 100 ms. At low levels of retinal illuminance the strongest motion signal is generated at ISI's of the order of 60 ms, and motion signals continue to be generated at very long ISI's. In computation of these responses, the sensor's delay Δ was set to 20 ms, and the temporal responses were computed as described by Sperling and Sondhi.[29]

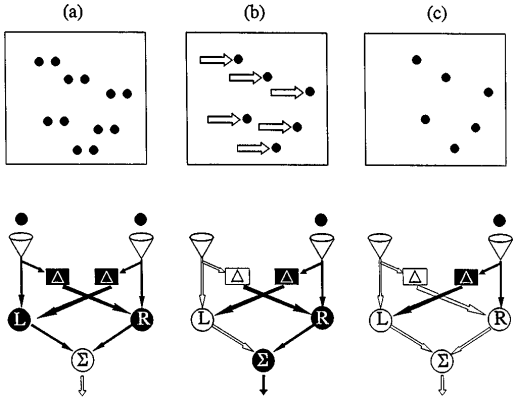

Fig. 9. Schematic representation of a rightward-motion sequence in the SIM paradigm. Filled sections indicate active elements. (a) Status of the motion sensor on presentation of the initial display containing the elements of both F1 and F2; inputs to the final stage Σ are balanced, and no motion signal is produced. (b) Status of the motion sensor when the elements in F1 are switched off while elements in F2 remain on view; the indirect input to correlator R remains active for the period of the sensor's delay Δ; this creates an imbalance at the input to the final stage Σ, and a rightward-motion signal is produced. (c) Status of the motion sensor some time $t > \Delta$ after F1 has been switched off while F2 remains on view; the inputs to the final stage are again balanced (zero), and no motion signal is produced.

with the effect of stimulus intensity, on the assumption of rapid light adaptation above background luminance.[12–14] As seen from Figs. 1 and 2, the performance curves for various levels of stimulus intensity are scaled versions of one another. We have been able to reproduce the scaling effect quite well, using an exponential function.

3. Motion with the SIM Paradigm

How a Reichardt sensor can signal rightward motion in the SIM paradigm is illustrated in Fig. 9. Figure 9(a) illustrates the status of the motion sensor during the initial period of the display sequence. Because the two inputs are activated simultaneously, left and right channels are balanced, and no motion signal is produced. Figure 9(b) shows the status of the sensor immediately after F1 has been switched off: after the direct input to correlator L has abated, the indirect input to correlator R remains active for the duration of the sensor's delay, Δ. The ensuing imbalance between left and right channels triggers a rightward motion signal. Figure 9(c) shows the status of the sensor some time $t > \Delta$ after F1 has been switched off: the two channels are again balanced, and no motion signal is produced.

As was done for the ISI paradigm, we implemented a computer simulation to illustrate a qualitative correspondence between the empirical results with the SIM paradigm and the response of the Reichardt motion sensor, activated as in Fig. 9. The parameters of the simulation were the same as for the ISI paradigm, except that only three levels of retinal illuminance were used: 1, 2, and 3 log Td. Unlike in the ISI simulation (Fig. 8), the curves for the SIM simulation, shown in Fig. 10, are monotonic. That is, having reached an asymptote, performance does not decline as the duration of F2 is increased. The simulated curves provide a good qualitative match to the empirical curves in Fig. 6. Quantitatively, one detail should be noted: the differences among the curves in rate of approach to asymptote is larger in the simulation than in the empirical data. The reasons for these differences are unclear but would have to be investigated before a fully quantitative model could be developed.

4. Cross-Paradigm Comparisons

The simulations in Figs. 8 and 10 are illustrative but do not provide an intuitively immediate description of the underlying processing events. A subsidiary qualitative account in terms of the motion sensor is presented below. To this end there are two aspects of the results in Figs. 3 and 6 that require elucidation. First, consider the shapes of the response curves: modulating the independent variable yielded nonmonotonic curves with the ISI paradigm (Fig. 3) but monotonic curves with the SIM paradigm (Fig. 6). In terms of the present model these differences arise because the two paradigms place different temporal constraints on the generation of motion signals. In both paradigms a motion signal is generated if the inputs to the final stage of the motion sensor Σ are unbalanced. In the ISI paradigm, maximum imbalance is reached at an optimal ISI dependent on the delay Δ; as ISI is increased beyond the optimal level, the imbalance diminishes, and the probability of a motion signal declines correspondingly. Thus the probability of seeing motion first increases up to an optimal ISI and then declines, as shown in Fig. 3. This issue can be illustrated if one refers to Fig. 7. In Fig. 7(b) the duration of the ISI is assumed to be optimal for generating a motion signal [Fig. 7(c)]. If the ISI is excessively long, the delayed signal arrives at correlator R during the ISI and has vanished by the time the direct input to R is activated; hence no motion signal is generated.

In the SIM paradigm the imbalance also reaches a maximum at an optimal duration of F2 dependent on Δ. And it is also true that the imbalance declines at longer

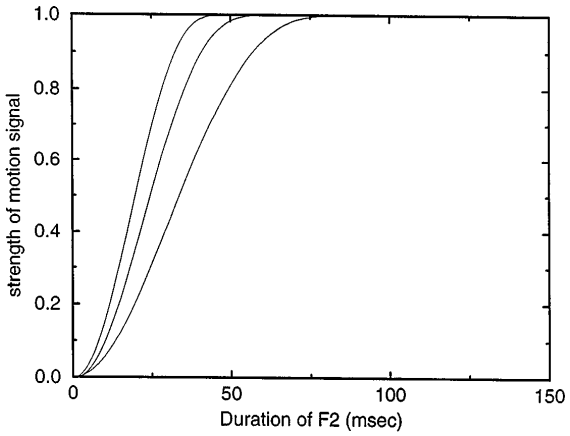

Fig. 10. Peak response of a Reichardt-type motion sensor to motion stimuli used in the SIM paradigm. In the computation the duration of the combined presentation of F1 and F2 was 1 ms, and the duration of the trailing frame, F2, was as indicated on the abscissa. Responses were computed for three levels of retinal illuminance: 10–1000 Td, in steps of 1 log unit. As the level of retinal illuminance is decreased, the strength of the motion signal reaches peak level at increasingly longer durations of F2. The parameters used in this simulation are the same as for Fig. 8.

durations of F2. But the decline is of no consequence because it occurs after the motion signal has been generated. That is, the continued presence of F2 beyond its optimal duration does not hinder the perception of motion for the simple reason that a motion signal has already been triggered by the offset of F1. This is illustrated in Fig. 9: the events shown in Fig. 9(c) can be extended in time indefinitely without interfering with the generation of the motion signal [Fig. 9(b)]. This produces the monotonic curves seen in Fig. 6.

A second cross-paradigm comparison concerns the effect of adapting luminance. Figure 3 shows that, at long SOA's, the probability of seeing motion was higher in dark-adapted than in light-adapted viewing. Congruent results have been reported in earlier investigations.[17–20] This effect is commonly explained on the assumption that the duration of the visual response is considerably longer in dark-adapted viewing.[29] In terms of the model illustrated in Fig. 7, the longer-lasting dark-adapted responses can produce motion signals over longer ISI's, thus yielding the results seen in Fig. 3.

By contrast, adapting luminance plays a negligible role at long durations of F2 in the SIM paradigm. As shown in Fig. 6, the probability of seeing motion remains high in both viewing conditions. This is to be expected because, given sufficient duration of F2, generation of a motion signal depends exclusively on F1 offset (see Fig. 9). To be sure, motion signals are likely to be triggered slightly sooner in light-adapted viewing because the visual responses are shorter; nevertheless, motion signals are produced also in dark-adapted viewing, if a little later.

2. METACONTRAST

A. Methods

As far as practicable, the metacontrast experiments were designed to parallel the motion experiments. The target stimulus was a 2°-square outline displayed in the center of the screen, with a 20-arcmin gap in the center of a randomly chosen side. The mask was a slightly larger square outline with a 20-arcmin gap in the center of each side. The separation between target and mask was 7 arcmin. The line thickness of target and mask was less than 1 arcmin.

Observers fixated a dim dot in the center of the screen and pressed a button an a hand-held box to start a trial. After each trial, observers indicated (or guessed) the side of the target that contained the gap (up, down, left, right) by pressing the appropriate response button. Metacontrast was studied with both the ISI and the SIM paradigms. In the ISI paradigm a variable ISI elapsed between F1 (the target) and F2 (the mask). In the SIM paradigm target and mask were displayed together for 1 ms; then the target was turned off, and the mask remained on view for a period that matched the duration of the ISI in the corresponding condition in the other paradigm. In both paradigms the intensity of the stimuli was varied over a wide range in both dark-adapted and light-adapted viewing. Luminance of the dots was set separately for each observer, as was done in the motion studies, so as to cover a range that yielded accuracy of performance from above chance to asymptotic levels.

B. Results

1. ISI Conditions

Results for the ISI light-adapted conditions (Fig. 11) revealed U-shaped masking curves for both observers. There was a tendency for the rate of recovery from masking to be related directly to stimulus luminance. In subsidiary trials we found that it took an SOA of at least 600 ms for performance with the dimmest stimuli to recover to the zero-SOA level. Optimal metacontrast occurred at an SOA of 40 ms at most luminances but at an SOA of 80 ms with very dim stimuli.

In contrast to the case of light-adapted viewing, little, if any, metacontrast masking was obtained under dark-adapted conditions (Fig. 12). A reduction in the magnitude of masking in dark-adapted viewing had been reported in earlier work[35]; however, we could find no other instances of the virtual abolition of masking as seen in Fig. 12. This discrepancy is likely to

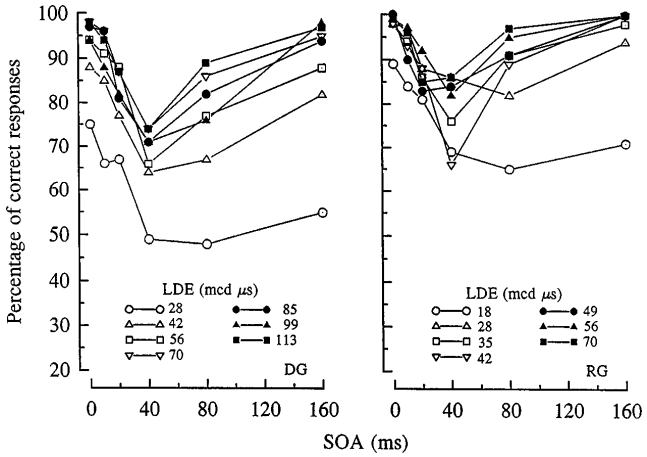

Fig. 11. Metacontrast task, ISI paradigm. Accuracy of gap-detection performance in light-adapted viewing for observers DG and RG. The duration of target and mask was 1 ms. Levels of stimulus intensity are shown in the legend. Chance level was 25%.

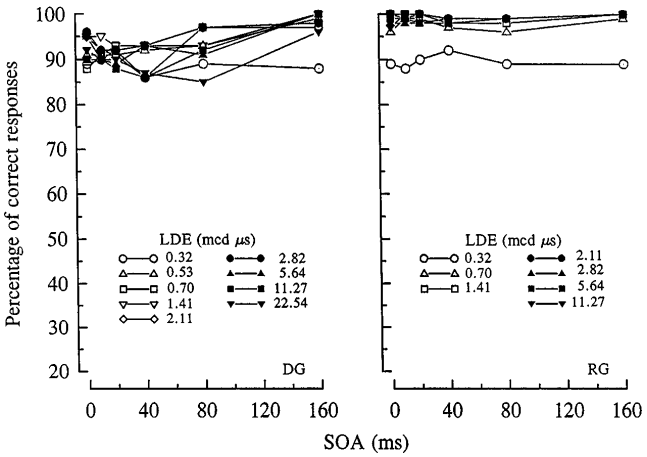

Fig. 12. Metacontrast task, ISI paradigm. Accuracy of gap-detection performance in dark-adapted viewing for observers DG and RG. The duration of target and mask was 1 ms. Levels of stimulus intensity are shown in the legend. Chance level was 25%.

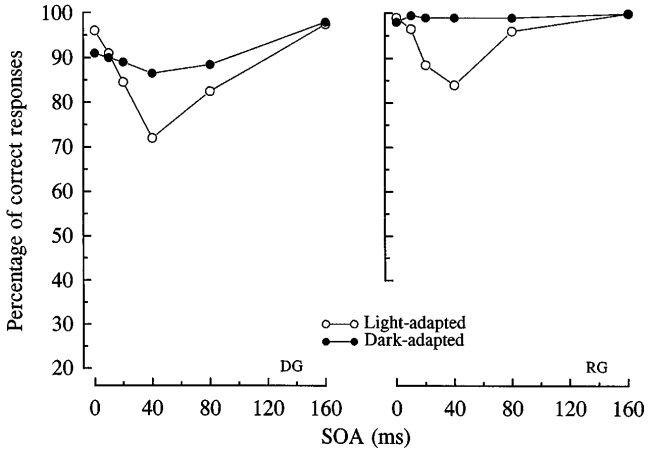

Fig. 13. Metacontrast task, ISI paradigm. Accuracy of gap-detection performance in light-adapted and dark-adapted viewing. Chance level was 25%. Each curve is the average of the results for the two highest stimulus intensities in light-adapted viewing (from Fig. 11) and in dark-adapted viewing (from Fig. 12) for observers DG and RG.

be related to the attribute of the target to which observers are required to respond. In all earlier studies in which metacontrast was investigated under both light-adapted and dark-adapted conditions, observers were required to report on the brightness or on the visibility of the target, not on its figural details. On the other hand, none of the studies that examined figural details of the target[36] was carried out under dark-adapted conditions.

An alternative, and not incompatible, account can be given in terms of the increased duration of the visual response under dark-adapted conditions. The visual response triggered by the target may be of such duration as to permit identification of the crucial figural detail, regardless of SOA. Thus, at intermediate SOA's (at which masking would occur in light-adapted viewing), target and mask would be temporally integrated and would be perceived as a single configuration. In a sense this result is homologous to that in Fig. 3 showing that motion can be seen over longer ISI's in dark-adapted than in light-adapted viewing: both outcomes can be explained in terms of the longer duration of the visual response under dark-adapted conditions.

A direct comparison of the results in light-adapted and dark-adapted viewing is presented in Fig. 13. Each curve in Fig. 13 is the average of the results for the two highest levels of stimulus luminance in light-adapted viewing (from Fig. 11) and in dark-adapted viewing (from Fig. 12), separately. The magnitude of metacontrast masking in light-adapted viewing is comparable with that obtained by Breitmeyer *et al.*[36] with a task based on detection of a figural detail of the target, much as in the present work. In dark-adapted viewing, only one observer (DG) showed a tendency toward a U-shaped performance curve. It is interesting to note that, in the ISI condition in the motion study (Figs. 1–3), the performance of the same observer decayed more rapidly than that of observer RG as a function of SOA. Taken together, the two sets of outcomes are consistent with the hypothesis that the visual responses of DG were shorter than those of RG.

2. SIM Conditions

Results for the SIM light-adapted conditions are shown in Fig. 14. The performance of both observers declined monotonically up to a mask duration of 160 ms. In subsidiary trials we found that the asymptotic performance shown in Fig. 14 declined only slightly at mask durations of 320 and 640 ms. The appearance of the displays was as in the ISI paradigm. Notably, the same impression of seeing the mask as though it were in expanding motion was experienced in both paradigms.

Figure 15 shows the results for the SIM dark-adapted conditions. Very little masking is evident with mask durations below 160 ms. The modest amount of masking seen at a mask duration of 160 ms was maintained at mask durations of 320 and 640 ms, as shown in subsidiary trials. It should be noted that, even at mask durations beyond 160 ms, no masking was ever obtained with very dim stimuli.

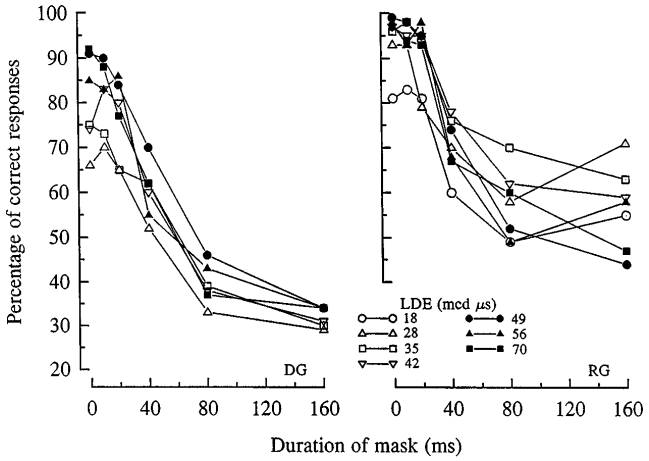

Fig. 14. Metacontrast task, SIM paradigm. Accuracy of gap-detection performance in light-adapted viewing for observers DG and RG. The duration of the combined target–mask display was 1 ms; the duration of the trailing-mask display indicated on the abscissas does not include the initial 1-ms period. Stimulus intensities are shown in the legend. Chance level was 25%.

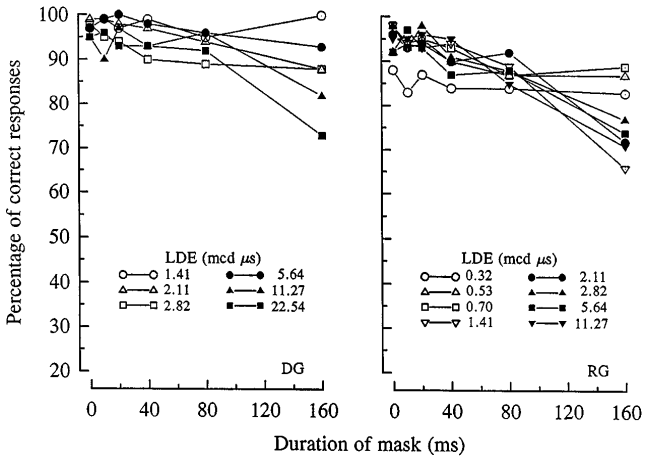

Fig. 15. Metacontrast task, SIM paradigm. Accuracy of gap-detection performance in dark-adapted viewing for observers DG and RG. The duration of the combined target–mask display was 1 ms; the duration of the trailing-mask display indicated on the abscissas does not include the initial 1-ms period. Stimulus intensities are shown in the legend. Chance level was 25%.

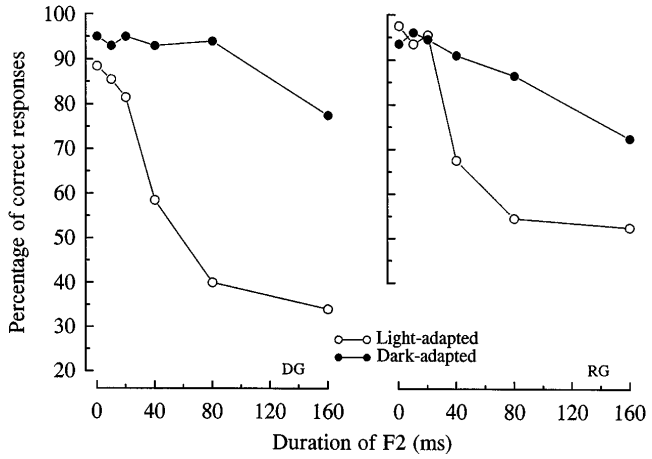

Fig. 16. Metacontrast task, SIM paradigm. Accuracy of gap-detection performance in light-adapted and dark-adapted viewing. Chance level was 25%. Each curve is the average of the results for the two highest stimulus intensities in light-adapted viewing (from Fig. 14) and in dark-adapted viewing (from Fig. 15) for observers DG and RG.

In keeping with the exposition used for the ISI paradigm, Fig. 16 shows a direct comparison of the results obtained in light-adapted and dark-adapted viewing. Each curve in Fig. 16 is the average of the results for the two highest levels of stimulus luminance in light-adapted viewing (from Fig. 14) and in dark-adapted viewing (from Fig. 15), separately. As mentioned above, the differences seen at a mask duration of 160 ms in Fig. 14 remained virtually unaltered at mask durations of 320 and 640 ms.

C. Discussion

1. Is It Metacontrast?

There is little question that the U-shaped curves obtained with the ISI paradigm represent metacontrast masking. Can the same be said for the monotonic curves obtained with the SIM paradigm? More generally, can the two paradigms be said to engage the same class of underlying mechanisms? We believe so. The two experiments had many similarities. The spatial configuration formed by target and masking stimuli was the same in both paradigms; and the dependent variable, detection of a discontinuity in the target's contour, was also held in common. The phenomenological appearance of the displays was very similar, and often indistinguishable, in the two paradigms. Unquestionably, masking was obtained with both paradigms; and the magnitude of masking was affected in similar ways by changes in adapting luminance. Individual differences between the two observers were maintained across paradigms: in light-adapted viewing, observer DG exhibited more masking than observer RG in both the ISI and the SIM (Figs. 13 and 16) paradigms.

But there were differences as well as similarities between the two sets of results. On comparison of Figs. 13 and 16, two differences are immediately obvious: in the shapes of the response curves and in the maximal amount of masking. First, let us consider the shapes of the response curves. The initial decrement in performance with the SIM paradigm is remarkably similar to the descending portion of the U-shaped curves with the ISI paradigm. Figures 13 and 16 show that levels of performance were very similar in the two paradigms but began to diverge at ~40 ms in light-adapted viewing. Beyond that, the recovery in performance with the ISI paradigm (Fig. 13) was a necessary consequence of the progressively longer mask delays: more processing of the target could be achieved as the duration of the mask-free (SOA) period was increased. By contrast, performance could not recover in the SIM paradigm because there was no mask-free period corresponding to the long SOA's.

Next, let us consider differences in maximal levels of masking. In the ISI paradigm light-adapted masking was maximal at an SOA of ~40 ms (Fig. 13). By contrast, in the SIM paradigm, strength of light-adapted masking continued to increase up to mask durations of at least 160 ms (Fig. 16). If it is true that the two paradigms reflect much the same masking processes, and if masking is triggered to its maximum level by the mask's presence on the screen some 40 ms after the onset of the target (as indexed by the ISI results), then the SIM performance curves should have declined to a minimum as mask duration was increased to ~40 ms and should have remained at that level for all longer mask durations. Why was that level exceeded at the longer mask durations in the SIM paradigm? It might be suggested that, since the mask remained on view, the SIM performance curves should represent the cumulative effect of the masking obtained at the corresponding SOA's in the ISI paradigm. Direct comparison of the relevant curves shows, however, that the magnitude of cumulative masking falls far short of the actual masking. Additional factors were probably at work in the SIM paradigm that magnified and extended the incidence of masking.

A more plausible supposition is that metacontrast masking may not be a unitary process. In his treatise on masking, Breitmeyer[3] (Chap. 8 and elsewhere) noted that metacontrast masking can take place at any or all of the first four hierarchical levels of processing proposed by Uttal.[37] Those processes involve (1) photoreceptor activity, (2) postreceptor neural interactions, (3) spatial and figural organization, and (4) contextual effects. Within this scheme a mask displayed at different SOA's is likely to interfere with processing at different levels and, in turn, to impair the perception of different attributes of the target.[38] In the present study a mask displayed at different SOA's in the ISI paradigm would interfere with some attributes of the target while leaving others unimpaired. On the other hand, fewer attributes of the target would be left unimpaired in the SIM paradigm because of the continued presence of the mask's contours alone throughout the period of processing. Specific ways in which masking might be accomplished are discussed in Subsections 2.C.2 and 2.C.3.

The objective of the preceding discussion was to decide whether the masking obtained with the ISI and with the SIM paradigms belong to the same class of perceptual events. Given the similarities noted at the beginning of this section, communality must be regarded as the default option. The arguments and the evidence reviewed above do little to disconfirm this working hypothesis.

2. Onset-Locked Fast Inhibition and Slow Excitation

Considering the nature of metacontrast masking, it is not surprising that inhibition has been used as an explana-

tory principle in several theoretical models. Perhaps the earliest model was that of Stigler,[3] which was based on inhibitory interactions at the level of the horizontal cells in the retina. Later models postulated inhibitory processes up to cortical levels.[35,39–41] A common problem encountered in these models is that masking is at maximum not at SOA = 0 but at longer SOA's up to 80–100 ms. How can a temporally trailing mask inhibit a target that preceded it by some 100 ms on the way to the visual cortex? A common solution has been to postulate that each stimulus, target and mask, generates two sets of responses: a fast inhibitory response and a slow excitatory response. In a metacontrast sequence, masking is said to occur over the range of SOA's at which the fast inhibitory component generated by the mask arrives at some higher center concurrently with the slow excitatory response generated by the target and inhibits it. Among the mechanisms that have been proposed are slow excitatory and fast inhibitory pathways in a neural network[41] and fast transient responses that inhibit slow sustained activity.[39]

Crucial to these theories—and their main weakness in accounting for the SIM results—is the assumption that both excitatory and inhibitory responses are time locked to stimulus onset. To be sure, the inhibitory component is said to be faster either because it travels along a faster pathway[41] or because it has a shorter latency.[39] But the excitatory and the inhibitory responses are assumed to be triggered simultaneously at stimulus *onset*. It follows from this assumption that no masking should occur if target and mask are displayed at SOA = 0. This is so because the fast inhibitory components of both stimuli will have come and gone before the slow excitatory components arrive at the higher center. In fact, all models in this family were designed to exclude masking effects at SOA = 0, so as to accommodate the finding that no metacontrast masking had ever been obtained in control conditions run at SOA = 0. In light of the present results, that result is easily understood. Earlier failures to obtain masking at SOA = 0 occurred because, in every case, target and masking stimuli not only started but also ended together. Thus SOA emerged as the critical variable, the SOA law was asserted, and models were developed to explain why an onset asynchrony was necessary for metacontrast masking. To the contrary, the present findings with the SIM paradigm demonstrate that the critical temporal asynchrony is not in the onset but in the termination of the stimuli.

Onset-locked inhibition is clearly ruled out as a source of masking in the SIM paradigm. An alternative inhibitory mechanism to be considered is offset-locked inhibition. It is known that the "off" response triggered by the termination of the mask can interfere with whatever processing of the target is still ongoing when the off response occurs.[42] As an account of the SIM results, however, this option is denied by the data. The reasoning is as follows: after an initial brief period of some tens of ms, which is required for the full development of an off response,[7,43] the effectiveness of the off response as a masking agent should diminish as the duration of the mask is increased. This is so because, as the duration of the mask is increased, the off response is progressively delayed, and correspondingly longer intervals become available for processing the target. In terms of performance (e.g., Fig. 16), this should result in a rapid development of masking at short mask durations followed by a steady recovery as the off response is progressively delayed at longer durations of the mask. No such recovery from masking is evident from Fig. 16. Indeed, Fig. 16 reveals the opposite trend: performance continued to decline as mask duration was increased. To dispel any doubts on this issue, we ran subsidiary trials in which mask duration was extended to several seconds, with the response curves showing no sign of recovery from an asymptote that was somewhat lower than the 160-ms level in Fig. 16. A mask-free interval of several seconds must be regarded as more than adequate for processing the contours of the target.

Failure to find evidence of masking by off responses may be due to any of several procedural differences between the present work and that of Breitmeyer and Kersey.[42] For instance, it is possible that the differences in outcomes are attributable to differences in response critera. Breitmeyer and Kersey used an apparent-brightness matching task, whereas we used a contour-discrimination task. Also, in the Breitmeyer–Kersey study the U-shaped masking function emerged only when the target disk and the surrounding mask ring were presented dichoptically (namely, to each eye separately). By contrast, in the present study all stimuli were presented binocularly (namely, to both eyes together). Whatever the reason for the different outcomes, the masking results obtained with the SIM paradigm (Fig. 16) must be ascribed to factors other than inhibitory interference arising from the mask's off response. Other accounts of those results are considered in Subsection 2.C.3.

3. *Bridgeman's Model of Metacontrast Masking*

The arguments presented in the preceding section were not intended to dismiss inhibition as a useful explanatory principle in metacontrast masking. There are at least two inhibition-based models that can account for the results obtained with the SIM paradigm. One is Matin's[44] model, which is presented in Section 3 in the context of a correlative analysis of motion and metacontrast. The other is Bridgeman's[45,46] model of distributed sensory coding based on lateral inhibitory interactions.

Bridgeman's model is couched in the activity produced by sequential stimuli in a cortical neural network. The tenets of the model, as well as the model's simulations of various aspects of metacontrast masking, have been reported in detail by Bridgeman.[45,46] It is assumed in the model that the salient processing activity takes place in the cortex—as distinct from the retina—within a layer of cells in which each unit has lateral inhibitory connections with neighboring units. Connections among the units are such that stimulation of one part of the network produces expanding waves of recurrent activity throughout the network. When external stimulation is turned off, network activity continues in an oscillatory fashion until it damps over a period of time. If two or more brief stimuli are presented in rapid succession, the total network activity consists of the summation of the persisting activity from stimuli early in the sequence with the activity initiated by each successive stimulus. It is assumed

that what an observer perceives at any given time depends on the pattern of ongoing network activity.

Metacontrast masking is handled as follows. When presented alone, the target and the mask each produce a unique pattern of spatiotemporal oscillations within the network. If the two are presented in close temporal succession, their characteristic activity patterns are summated into the total activity of the network. In this case, identification of the target depends on how well its characteristic pattern of activation can be extracted from total network activity. In Bridgeman's model, identification performance is predicted by means of a simple correlation between the pattern of activity produced by the target alone and that produced by the sequential presentation of target and mask. The higher the correlation, the greater the probability of a correct response.

Recurrent activity within the network is modeled in terms of modified Hartline–Ratliff equations.[47] The activity of any given cell in the network is given by the following equation[45]:

$$R_p(t) = e_p(t) - \sum_{j=1}^{n} k_{p,j}[R_j(t - |p - j|) - R_{p,j}{}^0], \qquad j \neq p, \tag{1}$$

where R_p is the firing rate of neuron p, R_j is the firing rate of neuron j, e_p is the excitatory input to p, $k_{p,j}$ is an inhibitory coefficient with a value $0 \leq k \leq 1$ expressing the effect of neuron j on neuron p, and $R_{p,j}{}^0$ is the corresponding inhibitory threshold. The term $p - j$ refers to the distance between neurons p and j. See Bridgeman[46] (p. 530) for further details.

In the simulation we followed Bridgeman's[45] procedures in every detail, notably in the timing of the oscillatory cycles. Separate simulations were run with ISI and with SIM sequences. The outcomes, shown in Fig. 17, are remarkably similar to the empirical curves in Figs. 13 and 16.

3. MOTION AND METACONTRAST

A. Concurrent Effects?

Motion perception and metacontrast masking have been linked, at least informally, ever since they have been studied experimentally. Early researchers reported a reduction in visibility of the temporally leading stimuli under conditions that produced motion perception.[3] Also, it was noted that masking is often accompanied by apparent motion from target to mask.[48–50]

Unquestionably, motion perception and metacontrast masking share many similarities. As we have noted, the two phenomena are often seen concurrently. It is worth emphasizing that, on the basis of phenomenological observations, masking of the temporally leading stimuli was obtained reliably in the motion sequences. That is, at the longer durations of F2 in the SIM motion sequences, the F1 stimuli were never perceived by the observers. Conversely, the perceptual suppression of the leading target in the metacontrast studies was accompanied by the subjective sensation of expanding motion. As to locus of stimulation, it was found in early investigations that both motion perception and metacontrast masking occur optimally when the stimuli are presented extrafoveally.[3] In a direct comparison, Kahneman[2] demonstrated that the two effects follow similar time courses and that performance in both cases is a U-shaped function of SOA. Conceptual links between the two phenomena have been proposed in several theoretical models reviewed below.

On the other hand, the concomitance of motion and metacontrast is not perfect. It has been shown that the similarities reported by Kahneman[2] are restricted to specific ranges of visual angle, luminance, and exposure duration; that is, the effects can be decoupled over other ranges of those variables.[51,52] Two further differences were noted by Kolers[53]: first, masking is obtained only at small spatial separations between target and mask, whereas motion continues to be seen at much wider separations. Second, masking depends critically on figural similarity between target and mask, but motion does not. Finally, metacontrast masking can be obtained even without apparent motion.[54] This finding has been confirmed by Reeves,[55] who showed strong metacontrast in conditions in which the target and mask were judged to be simultaneous. When they appeared to be simultaneous, no motion was apparent to the subject. Clearly, these results must be taken into account in the formulation of a general theory of motion and metacontrast.

B. Correspondence in the Present Study

We obtained good correspondence between motion and metacontrast under light-adapted but not under dark-adapted conditions. One possible reason for the failure of metacontrast masking under dark-adapted conditions has already been mentioned: the duration of dark-adapted visual responses might have been such as to permit temporal integration over much longer ISI's (or mask durations) than in light-adapted viewing. In turn, the target would have remained visible, either alone or integrated with the mask, for a period sufficient to permit detection of the contour gap. On the other hand, the possibility that inhibition might have played a role must not be overlooked. It has been known for some time that inhibition is much reduced or totally absent in the dark-adapted visual system.[33,56] Were metacontrast making—but not motion perception—to be dependent on inhibitory interactions, the dark-adapted results would follow. That is, the pattern of incidence of masking might be explained

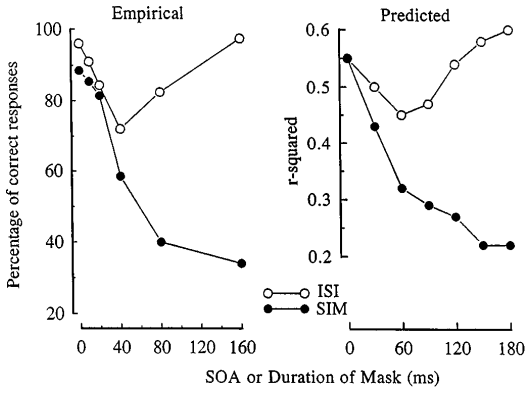

Fig. 17. Left-hand panel, empirical metacontrast results taken from Figs. 13 (ISI paradigm) and 16 (SIM paradigm). Right-hand panel, results of the simulation of Bridgeman's[45] distributed sensory coding model for metacontrast sequences of stimulation, for the ISI and the SIM paradigms.

in terms of the differential availability of inhibition in light-adapted and dark-adapted viewing. This option, however, must be considered *ad hoc*: it would require considerable elaboration to be a credible account of the total pattern of results.

Aside from the relationship between motion and metacontrast, an aspect of the results bearing on the relationship between the ISI and the SIM paradigms should be noted. In every case the two paradigms yielded homologous outcomes. To wit, in light-adapted viewing, both motion and masking were found with the ISI paradigm, and the same was true with the SIM paradigm. In dark-adapted viewing, the presence of motion and the absence of masking revealed in the ISI paradigm was again replicated in the SIM paradigm. Such a high degree of correspondence confirmed our confidence that the same perceptual processes, whether motion or metacontrast, were studied in the two paradigms.

C. Integrative Accounts

We noted above that metacontrast masking is unlikely to be a unitary process. Rather, the evidence suggests that masking can occur at more than one level and that its distinguishing characteristics may vary with the level at which it occurs. Much the same can be said for motion: it is unlikely that motion perception is a unitary phenomenon based on a single mechanism. Like masking, motion perception may be mediated by different mechanisms at distinct processing levels. Various suggestions have been made to distinguish among levels and mechanisms.[57–61]

A plausible corollary can now be proposed regarding the relationship between the two phenomena. If it is indeed the case that motion and metacontrast each can occur at more than one level, it is possible that they may co-occur at some levels but not at others. There is much evidence to suggest that co-occurrence may take place at early—but not at later—processing levels. On the basis of the outcome of earlier investigations,[2,51,52] Breitmeyer[3] concluded that "co-occurrence of metacontrast and stroboscopic motion prevails only at small spatial separations" (p. 122). In a more recent paper Breitmeyer[62] further suggested that reduction in the visibility of temporally leading stimuli is a property of the "short-range"[59,63] or "first-order"[60] motion system. The coupling of masking and low-level motion mechanisms is plausible in terms of the function commonly assigned to metacontrast masking: deblurring of motion smear.[35] It would obviously make sense for such deblurring to take place at low processing levels early in the sequence of visual information processing.

Assuming for the moment that masking and low-level motion are functionally coupled, what remains to be determined is how the coupling is achieved. Two separate—though not mutually exclusive—principles have been suggested: inhibition and spatiotemporal integration. In either case individual proposals have been somewhat general: formal models of the relationship between motion and masking have not been developed. In some inhibitory theories the mechanisms of inhibition are specified in some detail,[39–41] but the linkage between motion and masking is unspecified, even through masking is said to deblur motion smear. In the case of Matin's[44] proposal, the two phenomena are linked explicitly: masking is said to occur when a motion signal is produced; but the coupling mechanisms remain unspecified.

In another class of theories masking is also said to be a consequence of the activation of motion sensors.[49,54,64–66] In these theories the mechanism of masking is not inhibition but a spatiotemporal fusion between target and mask. The target's activity is said to become assimilated by that of the mask in a process reminiscent of the "plastic transformations" described by Kolers[53] when motion is seen between two objects of different shapes. A plausible neurophysiological mechanism capable of mediating spatiotemporal integration of successive stimuli has been proposed by Burr *et al.*[65] in terms of "spatiotemporal receptive fields," frequency tuned in both space and time. In principle, metacontrast masking can be explained in terms of the activation of such receptive fields by the sequential presentation of target and mask. In the words of Burr *et al.* (Ref. 65; p. 262), "These fields do not report the separate locations of the successively presented stimuli, but the *Gestalt* of a single [stimulus] in motion. The two separate presentations become perceptually merged." Burr *et al.*[65] acknowledge that this explanation is incomplete: what is missing is a description of the role played by a Reichardt-type motion sensor—said to produce the required motion signal[64]—in the summation of target and mask.

In summary, sufficient evidence is available to justify the working hypothesis that metacontrast masking is probably associated with the activity of low-level motion sensors. Indeed, as noted by Burr,[64] the association is almost inescapable: at the input site of any given motion sensor the spatiotemporal distribution of energy produced by a motion stimulus is the same as that produced by a metacontrast stimulus. The conceptual framework necessary to test this working hypothesis, however, is yet to be developed. As noted above, the options of inhibitory interactions and spatiotemporal summation need not be regarded as mutually exclusive. In addition, other formulations[55,67] must also be taken into account if a general theory of motion and metacontrast is to be developed.

ACKNOWLEDGMENTS

This work was supported by grants OGP0006592 and OGP38521 from the Natural Sciences and Engineering Research Council of Canada to V. Di Lollo and W. F. Bischof, respectively.

Correspondence may be addressed to either author at the Department of Psychology, University of Alberta, Edmonton, Alberta T6G 2E9, Canada.

REFERENCES

1. D. Kahneman, "Method, findings, and theory in studies of visual masking," Psychol. Bull. **70,** 404–425 (1968).
2. D. Kahneman, "An onset-onset law for one case of apparent motion and metacontrast," Percept. Psychophys. **2,** 577–584 (1967).
3. B. G. Breitmeyer, *Visual Masking: An Integrative Approach* (Oxford U. Press, New York, 1984).
4. V. Di Lollo, W. F. Bischof, and P. Dixon, "Stimulus-onset asynchrony is not necessary for motion perception or metacontrast masking," Psychol. Sci. **4,** 260–263 (1993).

5. G. Finley, "A high-speed point plotter for vision research," Vision Res. **25,** 1993–1997 (1985).
6. G. Sperling, "The description and luminous calibration of cathode ray oscilloscope visual displays," Behav. Res. Methods Instrum. **3,** 148–151 (1971).
7. J. Servière, D. Miceli, and Y. Galifret, "A psychophysical study of the visual perception of 'instantaneous' and 'durable'," Vision Res. **17,** 57–63 (1977).
8. V. Di Lollo and G. Finley, "Equating the brightness of brief visual stimuli of unequal durations," Behav. Res. Methods Instrum. Comput. **18,** 582–586 (1986).
9. P. Dixon and V. Di. Lollo, "Beyond visible persistence: an alternative account of temporal integration and segregation in visual processing," Cogn. Psychol. **26,** 33–63 (1994).
10. C. W. Eriksen and J. F. Collins, "Some temporal characteristics of visual pattern perception," J. Exp. Psychol. **74,** 476–484 (1967).
11. J. W. Onley and R. M. Boynton, "Visual responses to equally bright stimuli of unequal luminance," J. Opt. Soc. Am. **52,** 934–940 (1962).
12. M. M. Hayhoe, N. I. Benimoff, and D. C. Hood, "The time course of multiplicative and subtractive adaptation process," Vision Res. **27,** 1981–1996 (1987).
13. D. C. Hood and M. A. Finkelstein, "Sensitivity to light," in *Handbook of Perception and Human Performance,* K. Boff, L. Kaufman, and J. Thomas, eds. (Wiley, New York, 1986), pp. 5.1–5.66.
14. J. J. Koenderink, W. A. van de Grind, and M. A. Bouman, "Foveal information processing at photopic luminances," Kybernetik **8,** 128–144 (1971).
15. R. Groner, M. T. Groner, P. Müller, W. F. Bischof, and V. Di Lollo, "On the confounding effects of phosphor persistence in oscilloscopic displays," Vision Res. **33,** 913–917 (1993).
16. M. M. Hayhoe, "Spatial interactions and models of adaptation," Vision Res. **30,** 957–965 (1990).
17. M. Dawson and V. Di Lollo, "Effects of adapting luminance and stimulus contrast on the temporal and spatial limits of short-range motion," Vision Res. **30,** 415–429 (1990).
18. M. J. Morgan and R. Ward, "Conditions for motion flow in dynamic visual noise," Vision Res. **20,** 431–435 (1980).
19. C. Bonnet, "Threshold of motion perception," in *Tutorials in Motion Perception,* A. W. Wertheim, W. A. Wagenaar, and H. W. Leibowitz, eds. (Plenum, New York, 1982), pp. 41–79.
20. F. L. van Nes, J. J. Koenderink, H. Nas, and M. A. Bouman, "Spatio-temporal modulation transfer in the human eye," J. Opt. Soc. Am. **57,** 1082–1088 (1967).
21. F. W. Campbell and L. Maffei, "The influence of spatial frequency and contrast on the perception of moving patterns," Vision Res. **21,** 713–721 (1981).
22. O. Braddick, "The masking of apparent motion in random-dot patterns," Vision Res. **13,** 355–369 (1973).
23. W. Reichardt, "Autocorrelation, a principle for the evaluation of sensory information," in *Sensory Communication,* W. A. Rosenblith, ed. (MIT Press, Cambridge, Mass., 1961), pp. 303–317.
24. E. H. Adelson and J. R. Bergen, "Spatiotemporal energy models for the perception of motion," J. Opt. Soc. Am. A **2,** 284–299 (1985).
25. J. P. H. van Santen and G. Sperling, "Elaborated Reichardt detectors," J. Opt. Soc. Am. A **2,** 300–320 (1985).
26. V. Di Lollo, "Temporal integration in visual memory," J. Exp. Psychol. Gen. **109,** 75–97 (1980).
27. V. Di Lollo, J. H. Hogben, and P. Dixon, "Temporal integration and segregation of brief visual stimuli: patterns of correlation in time," Percep. Psychophys. **55,** 373–386 (1994).
28. J. Duysens, G. A. Orban, J. Cremieux, and H. Maes, "Visual cortical correlates of visible persistence," Vision Res. **25,** 171–178 (1985).
29. G. Sperling and M. M. Sondhi, "Model for visual luminance discrimination and flicker detection," J. Opt. Soc. Am. **58,** 1133–1145 (1968).
30. M. Ikeda, "Temporal summation of positive and negative flashes in the visual system," J. Opt. Soc. Am. **55,** 1527–1534 (1965).
31. D. H. Kelly, "Theory of flicker and transient responses. I. Uniform fields," J. Opt. Soc. Am. **61,** 537–546 (1971).
32. D. H. Kelly, "Theory of flicker and transient responses. II. Counterphase gratings," J. Opt. Soc. Am. **61,** 632–640 (1971).
33. G. von Békésy, "Mach- and Hering-type lateral inhibition in vision," Vision Res. **8,** 1483–1499 (1968).
34. J. E. Farrell, M. Pavel, and G. Sperling, "The visible persistence of stimuli in stroboscopic motion," Vision Res. **30,** 921–936 (1990).
35. M. Alpern, "Metacontrast," J. Opt. Soc. Am. **43,** 648–657 (1953).
36. B. G. Breitmeyer, R. Love, and B. Wepman, "Contour suppression during stroboscopic motion and metacontrast," Vision Res. **14,** 1451–1456 (1974).
37. W. R. Uttal, *A Taxonomy of Visual Processes* (Erlbaum, Hillsdale, N.J., 1981).
38. M. C. Williams and N. Weisstein, "The effect of perceived depth and connectedness on metacontrast functions," Vision Res. **24,** 1279–1288 (1984).
39. B. G. Breitmeyer and L. Ganz, "Implications of sustained and transient channels for theories of visual pattern masking, saccadic suppression, and information processing," Psychol. Rev. **83,** 1–36 (1976).
40. N. Weisstein, "A Rashevsky–Landahl neural net: stimulation of metacontrast," Psychol. Rev. **75,** 494–521 (1968).
41. N. Weisstein, "Metacontrast," in *Handbook of Sensory Physiology,* D. Jameson and L. M. Hurvich, eds. (Springer-Verlag, New York, 1972), Vol. 7/4, pp. 233–272.
42. B. G. Breitmeyer and M. Kersey, "Backward masking by pattern stimulus offset," J. Exp. Psychol. Human Percept. Perf. **7,** 972–977 (1981).
43. M. Ikeda and R. M. Boynton, "Negative flashes, positive flashes, and flicker examined by increment threshold technique," J. Opt. Soc. Am. **55,** 560–566 (1965).
44. E. Matin, "The two-transient (masking) paradigm," Psychol. Rev. **82,** 451–461 (1975).
45. B. Bridgeman, "Distributed sensory coding applied to simulation of iconic storage and metacontrast," Bull. Math. Biol. **40,** 605–623 (1978).
46. B. Bridgeman, "Metacontrast and lateral inhibition," Psychol. Rev. **78,** 528–539 (1971).
47. F. Ratliff, *Mach Bands: Quantitative Studies on Neural Networks in the Retina* (Holden-Day, San Francisco, Calif., 1965).
48. E. Fehrer and E. Smith, "Effects of luminance ratio on masking," Percept. Mot. Skills **14,** 243–253 (1962).
49. P. H. Schiller and M. C. Smith, "A comparison of forward and backward masking," Psychonom. Sci. **3,** 77–78 (1965).
50. H. Werner, "Studies on contour: I. Qualitative analysis," Am. J. Psychol. **47,** 40–64 (1935).
51. B. G. Breitmeyer and K. Horman, "On the role of stroboscopic motion in metacontrast," Bull. Psychonom. Soc. **17,** 29–32 (1981).
52. N. Weisstein and R. Growney, "Apparent movement and metacontrast: a note on Kahneman's formulation," Percept. Psychophys. **5,** 321–328 (1969).
53. P. A. Kolers, *Aspects of Motion Perception* (Pergamon, New York, 1972).
54. A. E. Stoper and S. Banffy, "Relation of split apparent motion to metacontrast," J. Exp. Psychol. Human Percept. Perf. **3,** 258–277 (1977).
55. A. Reeves, "Pathways in type-B (U-shaped) metacontrast," Perception **15,** 163–172 (1986).
56. H. B. Barlow, R. Fitzhugh, and S. W. Kuffler, "Dark adaptation, absolute threshold and Purkinje shift in single units of the cat's retina," J. Physiol. (London) **137,** 327–337 (1957).
57. E. H. Adelson and J. A. Movshon, "Phenomenal coherence of moving visual patterns," Nature (London) **300,** 523–525 (1982).
58. W. F. Bischof and V. Di Lollo, "Perception of directional sampled motion in relation to displacement and spatial frequency: evidence for a unitary motion system," Vision. Res. **30,** 1341–1362 (1990).
59. O. Braddick, "Low-level and high-level processes in apparent motion," Philos. Trans. R. Soc. London Ser. B **290,** 137–151 (1980).
60. P. Cavanagh and G. Mather, "Motion: the long and short of it," Spatial Vis. **4,** 103–129 (1989).

61. C. Chubb and G. Sperling, "Drift-balanced random stimuli: a general basis for studying non-Fourier motion perception," J. Opt. Soc. Am. A **5,** 1986–2007 (1988).
62. B. G. Breitmeyer, "On visual masking and motion," presented at the Conference on Neurophysiological Foundations of Visual Perception, Badenweiler, Germany, July 1987.
63. O. Braddick, "A short-range process in apparent motion," Vision Res. **14,** 519–527 (1974).
64. D. C. Burr, "Summation of target and mask metacontrast stimuli," Perception **13,** 183–192 (1984).
65. D. C. Burr, J. Ross, and M. C. Morrone, "Seeing objects in motion," Proc. R. Soc. London Ser. B **227,** 249–265 (1986).
66. E. Fehrer, "Effects of stimulus similarity on retroactive masking," J. Exp. Psychol. **71,** 612–615 (1966).
67. L. Ganz, "Temporal factors in visual perception," in *Handbook of Perception,* E. C. Carterette and M. P. Friedman, eds, (Academic, New York, 1975), Vol. 5, pp. 169–231.